Isotopic identification of special nuclear materials based on the delayed γ rays from photofission fragments*

M.Z. Wang,[1,2,3] H.Y. Lan,[2,3] D. Wu,[2,3] X.L. Xu,[2,3] R.R. Xu,[4] X.Q. Yan,[2,3,†] and W. Luo[1,‡]

[1]*School of Nuclear Science and Technology, University of South China, Hengyang 421001, China*
[2]*State Key Laboratory of Nuclear Physics and Technology,*
School of Physics, CAPT, Peking University, Beijing 100871, China
[3]*Beijing Laser Acceleration Innovation Center, Beijing 101407, China*
[4]*China Nuclear Data Center, China Institute of Atomic Energy, Beijing, 102413, China*

The illicit trafficking of Special Nuclear Materials (SNMs) poses a grave threat to global security, necessitating the development of effective nuclear material identification methods. This paper investigates a method to isotopically identify the SNMs, including ^{233,235,238}U, $^{239-242}$Pu, and ^{232}Th, based on the detection of delayed γ rays from photofission fragments. The delayed γ ray spectra resulting from the photofission of the SNMs under the irradiation of a 14 MeV γ beam with a total number of 10^9 are simulated with Geant4. Three high-yield fission fragments, i.e., ^{138}Cs, ^{89}Rb, and ^{94}Y, are selected as the candidate fragments for SNM identification. The yield ratios of these three fragments are calculated and the results from different SNMs are compared against each other. It is found that yield ratio of ^{138}Cs/^{89}Rb can be used to distinguish most of the SNMs, including ^{233,235,238}U, ^{242}Pu, and ^{232}Th, with a high confidence level above 95%. To achieve the discrimination of $^{239-241}$Pu with the same confidence, a higher total number of 10^{11} γ beam is required. Moreover, the ^{94}Y/^{89}Rb ratio can be used to identify these SNMs elementally, but the isotopic identification is difficult. Additionally, using the count rate of the delayed γ above 3 MeV, the presence of nuclear materials can be rapidly distinguished within a few seconds.

Keywords: Special nuclear material identifications, Photofission, Active interrogation, Yield ratio

I. INTRODUCTION

The illicit proliferation of special nuclear materials (SNMs) is a crucial way for terrorists to acquire weapons of mass destruction. Generally, the conventional scanning systems deployed at national borders use X-rays to obtain the scanned object's density distribution, which cannot differentiate SNMs from other high-density metals such as lead, tungsten, and bismuth. Therefore, many efforts are made to realise the on-site, nondestructive identification of SNMs. Detection methods of SNMs can be categorised as passive and active interrogation. Passive interrogation relies on detecting naturally emitted γ rays or neutrons from the radioactive decay of SNMs [1–4]. However, this technique is unsuitable for detecting shielded objects, as the intensities and energies of spontaneous radiation are relatively low. Active interrogation, on the other hand, employs an external radiation source and can effectively overcome such limitations. An optimal response can be achieved by adjusting the energy and intensity of the interrogation radiation source. The primary interrogation radiations are neutrons, muons, and photons. Neutron fission reactions with fissile material have the advantage of high penetrability and high cross sections, leading to extensive research [5–8]. However, neutrons are hard to handle in the context of radiation safety and neutron sources induce neutron capture reactions in nearly all materials, resulting in additional radiation background and increasing difficulties in signal discrimination. Furthermore, neutron generation devices, such as spallation neutron sources or nuclear reactors, typically require a large area and are thus unsuitable for widespread applications. The muon scattering tomography technology based on cosmic-ray muons for detecting SNMs has also attracted extensive research [9–11]. Nevertheless, the muon generation devices are complex, costly, and unsuitable for broad usage. Photons are often preferred over neutrons and muons, due to their lower induction of radioactivity in most materials. By far, photon-induced reactions can not only detect explosives [12] but identify SNMs based on nuclear resonance fluorescence(NRF) [13–15]. However, the resonance width of NRF reactions is very narrow ($\sim$meV), which requires γ-ray sources with high spectral and temporal intensity to gain sufficient signals within a reasonable irradiation time. These obstacles make the development of SNM detection methods based on photofission indispensable.

Photofission is a process in which a fissile nucleus splits into two fragments (light and heavy) after absorbing an incident photon. At the very instant fission fragments are generated, prompt neutrons and prompt γ rays are emitted, and then the radioactive fragments decay into stable nuclides, releasing delayed γ rays. As the thresholds for most photonuclear reactions are generally above 7 MeV, the background radiation from photofission tends to be relatively low. Currently, most identification of SNMs research based on photofission focused on the ^{235,238}U, and ^{239}Pu. Their work focuses on identifying and quantitatively analyzing some nuclides [16–20], and constructing an analysis algorithm for the delayed γ energy spectrum of SNMs in simulations [21, 22]. Additionally, using delayed γ-ray ratios for SNM differentiation, which was first proposed by Hollas *et al.* [23] has re-

ceived much attention. Finch *et al.* [24] utilized three high-purity germanium (HPGe) detectors to distinguish ^{235,238}U and ^{239}Pu. Nevertheless, the high costs and neutron damages of HPGe detectors make them susceptible during fission reactions, posing challenges for repeated implementation and practical applications of this method. Therefore, a detection method that can be widely applied for more isotopes holds greater significance. Methods for the identification of a broader range of SNMs including ^{233,235,238}U, $^{239-242}$Pu, and ^{232}Th are required. It is crucial to consider the existence and identification of additional isotopes of U, Pu, and Th to effectively manage SNMs.

Meanwhile, with the rapid developments of high-intensity γ-ray facilities in China, new opportunities have opened up for photofission research. Recently, the Shanghai Laser Electron Gamma Source beamline at the Shanghai Synchrotron Radiation Facility has been completed and is in operation, providing more platforms for fields such as photonuclear physics [25, 26]. Moreover, laser-driven γ ray sources can reach extremely high intensities and offer the advantage of wide range energies, γ rays with intensities above 10^{19}/s (10^8/shot, above 4 MeV) were generated using the 200 TW laser facility at the Compact Laser Plasma Accelerator (CLAPA) Laboratory [27], where significant photonuclear researches have been conducted in our previous studies [28–33]. Laser-driven γ ray sources can be much more miniaturised and are well-suited for widespread use in customs and railway security. These emerging quasi-monoenergetic γ source devices [34, 35] and high-intensity γ-ray facilities will provide broad application prospects for photofission research and its application in SNM identification.

In this work, we systematically investigate the identification methods to identify the elements and isotopes of SNMs by detecting delayed γ rays from photofission fragments. Geant4 [36] simulations are performed on the photofission of the SNM isotopes, including ^{233,235,238}U, $^{239-242}$Pu, and ^{232}Th. To identify potential fragment ratios that can be used in SNM identification, the mass and charge yield distributions of photofission fragments induced by monochromatic γ source and their delayed γ spectrum recorded by an HPGe detector are obtained. According to the delayed γ spectrum, the yields of fission fragments are calculated. The ratios of three high-yield fission fragments, ^{138}Cs, ^{94}Y, and ^{89}Rb, are selected as identification values for differentiating these SNMs. The dependence of the fragment ratios on incident γ-ray energy is also investigated. Moreover, the count rates of delayed γ rays with energies above 3 MeV recorded by a LaBr$_3$ detector are calculated and used to rapidly distinguish whether the scanned object contains nuclear material. This comprehensive approach will provide a better understanding and control of SNMs.

II. METHOD

The fission fragments of different fissile nuclei exhibit variations, the charge and mass yield distributions shift towards larger masses as the mass of the fissile nucleus increases.

Hence, it is plausible to employ the yield ratios of fission fragments as an identification parameter for distinguishing different fission nuclei. In reality, the fragment yields have to be calculated from the detected delayed γ ray spectra according to parameters such as the delayed γ-ray intensity, detection efficiency, and attenuation in the target. Consequently, the simulation of the delayed γ rays detection would help to gain insight into SNMs identification.

To simulate the detection of delayed γ rays from photofission fragments, the Geant4 photofission module developed by our lab is employed [37, 38]. In this module, the mass and charge yield distribution of fission fragments is based on the Bohr-substitution Gorodisskiy model [38, 39]. It can describe the characteristics of photofission reaction products from actinides, such as prompt neutrons, prompt photons, and fission fragments. The results have been extensively benchmarked against the available experimental data, which showed good agreement. Additionally, to model the delayed γ emission from fission fragments, the G4RadioactiveDecay physics is implemented in our code. These modules are instrumental in simulating the photofission process of SNMs within the scope of this study.
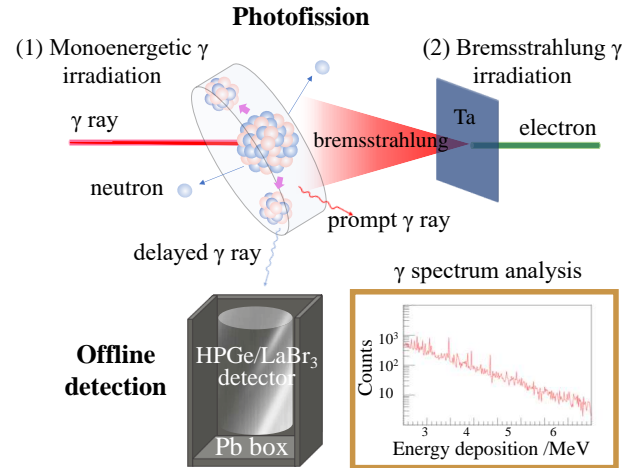

Fig. 1. The schematic diagram for the offline detection of delayed γ rays from the radioactive decay of SNM photofission fragments. Either (1) a monoenergetic γ source or (2) a bremsstrahlung source generated from the interaction between the electron beam and Ta was used to perform the simulations. The γ-ray source irradiates the target, which induces photofission of the SNMs to be inspected. The resulting radioactive fission fragments would emit γ rays during decay. An HPGe or a LaBr$_3$ detector records the characteristic γ-delayed peaks from fission fragments in a low-background lead chamber.

The illustration of the simulation setup is shown in Fig. 1. The monoenergetic γ source or the bremsstrahlung γ source are incident at an oblique angle of $45°$ upon eight types of SNM targets, each with a thickness of 1 cm, resulting in photofission reactions. A LaBr$_3$ detector, with a size of $8*16$ cm, is placed perpendicular to the γ beam and in parallel to the target to detect the γ rays. LaBr$_3$ detectors have high detection efficiency, and the count rate of the fission γ rays
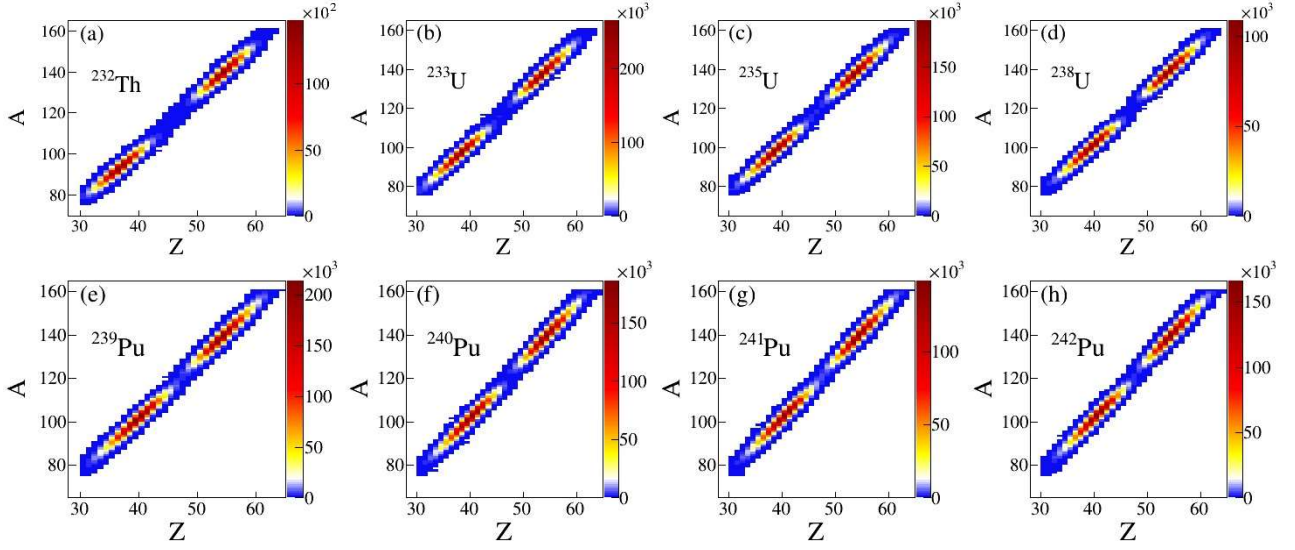
Fig. 2. The mass and charge yield distribution of fission fragments of ^{233,235,238}U, $^{239-242}$Pu, ^{232}Th.

above 3 MeV can be obtained, which can serve as an instant indicator of the presence of SNMs. HPGe detectors, which have high resolution, are suitable to measure and analyze the peak structure of complex delayed γ spectrum. Five minutes after the fission reaction, the HPGe detector, with a relative efficiency of 80%, is placed to detect the delayed γ rays from fragments. In the delayed γ spectrum of photofission products measured by an HPGe detector, one can determine the counts of characteristic γ peak of most high-yield product nuclides. The yields of fission fragments can be calculated with the γ ray counts, detection efficiency simulations, and self-absorption corrections. The yield ratio is regarded as an identification characteristic for differentiating SNMs. It can be obtained by screening the most differentiated identification values of each SNM and their uncertainties. Moreover, the count rates of delayed γ rays with energies above 3 MeV were used to distinguish whether it is nuclear material or not rapidly.

The fragment yields are determined by factors such as incident photon energy, beam intensity, target nucleus number, and photofission cross-section. The fission of a heavy nucleus predominantly produces six hundred to eight hundred different isotopic fragment species. Therefore, it's crucial to carefully select the fission fragments with high yields, measurable half-lives, and significant counts of delayed γ rays. To optimize the yields of fission products, referring to the information on photofission cross-section in TENDL-2019 [40], a monoenergetic γ source with energies around 14 MeV was selected as it offers almost the maximum cross-sections for uranium, plutonium, and thorium. 10^9 incident γ rays were employed for the isotopes of uranium and plutonium, and thorium in Geant4 simulations. Regarding measurable half-lives, the minute order to hour order is suitable for detection. In

conclusion, through the identification of characteristic values presented herein, we have determined the yield ratios associated with each unique fission nucleus exhibiting notable differentiation from other fission nuclei.

III. RESULTS

A. Mass and charge Yield Distribution

Fig. 2 illustrates the mass and charge yield distribution of fission fragments from the eight selected SNMs at the incident γ-ray energy of 14 MeV. The number of neutrons in fission fragments is between 40 and 90, and the proton number is from 25 to 65. Generally, the nuclides located in the two peak areas of the figures represent the high-yield fragments, with the proton numbers of lighter fragments concentrated mostly between 36 and 46, and the proton numbers of heavier fragments concentrated within 50-60. Differences in high-yield fragments among U, Pu, and Th are found observable, as shown in Fig. 2. Fig. 2(b-d) shows that the overall fragment yield drops as the target mass number increases for the isotopes of ^{233,235,238}U. For $^{239-242}$Pu isotopes, the decrease of fragment yields with target mass number shows less linearity, as shown in Fig. 2(e-h). Moreover, the mass and charge yield distributions also show discrepancies among the eight selected isotopes. Such features indicate that the fragment yields and ratios can be utilized to discriminate between the SNMs. After a thorough analysis of these mass and charge yield distributions, we identified a preliminary candidate list of high-yield fragments that might be suitable for use in further SNM discrimination: ^{86}Se, ^{89}Rb, ^{94}Y, ^{95}Y, ^{98}Y, ^{102}Nb, ^{129}Sb, ^{132}I, ^{132}Cs, ^{138}Cs, and ^{138}Xe. These high-yield frag-

TABLE 1. The information of fragment nuclides for identification. Fragments for identification are the product nuclides finally selected for SNMs identification. Parent Nucleus are the fission fragments which would decay into the fragments for identification in the detection time. Productivity of fragments for identification is yield which is obtained by the peak in the γ decay spectrum divided by the total incident γ flux. The productivity of the parent nucleus is the yield obtained from simulation divided by the total incident γ flux. All the productivity values are the data when ^{233}U is used as the reaction target.

Fragments for identification	γ Energy (Branch)	Parent Nucleus	Half-life	Decay Mode(Branch)	Productivity (‰)
^{138}Cs	1435.77 keV (76.3%)		32.84 min		0.527812
		^{138}Xe	14.14 min	$\beta-$ (100%)	0.000222
		^{138}I	6.303 s	$\beta-$ (100%)	0.000181
		^{138}Te	1.46 s	$\beta-$ (100%)	0.000018
		^{138}Sb	314 ms	$\beta-$ (100%)	0.0000002
^{89}Rb	1031.92 keV (63%)		15.39 min		0.451795
		^{89}Br	4.348 s	$\beta-$ (100%)	0.000067
		^{89}Se	0.41 s	$\beta-$ (100%)	0.000139
		^{89}Se	1.51 s	$\beta-$ (100%)	0.000063
		^{89}As	200 ms	$\beta-$ (100%)	0.000003
^{94}Y	918.74 keV (56%)		18.7 min		0.706307
		^{94}Sr	75.3 s	$\beta-$ (100%)	0.000120
		^{94}Rb	2.704 s	$\beta-$ (100%)	0.000241
		^{94}Kr	212.0 ms	$\beta-$ (100%)	0.000115
		^{94}Br	70.0 ms	$\beta-$ (100%)	0.000006

ments were selected from the mass and charge yield distribution as preliminary screening results, providing support for the subsequent search for characteristic peaks in the complex delayed γ spectrum and serving as a basis for choosing the measurement time of the HPGe detector.

B. delayed γ-ray Spectrum

The typical delayed γ-ray spectra from the fission fragment of ^{233}U, ^{239}Pu, and ^{232}Th, recorded by the HPGe detector are shown in Fig. 3. Gamma spectra with energy below 511 keV are rather complex due to characteristic peaks from multiple sources and thus are not considered in the analysis. The data acquisition time is set from 5 minutes to 1 hour after the irradiation. As shown in Fig. 3(a-c), the energy of the delayed γ signals mostly lies in the region below 4 MeV. The corresponding characteristic peak counts of fission fragments range from a few hundred to over a thousand, which have good statistical errors within the achievable γ source flux. The detection efficiency of high energy γ above 4 MeV is low and thus is not shown or analyzed in detail.

After the initial screening of candidate fragment nuclides, the secondary screening requires that the source of the characteristic peak is clean (with no other characteristic peaks present within 1 keV) and that the counts in different fission nuclei exhibit significant differences. For instance, γ peak 667.714 keV of the ^{132}I has the same energy as the γ peak 667.714 keV of ^{132}Cs (see Fig. 3(d-f)), which is close to the γ peak 668.536 keV of ^{130}I. All three fragment nuclides have relatively high yields and non-negligible characteristic peak counts. When the detector's resolution is insufficient, the overlapping of these neighbouring peaks will impact the fragment yield determination. Moreover, although the characteristic peaks of the candidate fragments such as ^{95}Y and ^{129}Sb have relatively large signals, their net counts show no significant difference among the eight SNMs. Therefore, these characteristic peaks, marked with black tags at the top of Fig. 3, were not usable as identification fragments. After filtering out these unusable candidate signals, three fragments, ^{94}Y, ^{89}Rb, and ^{138}Cs, are identified as the usable fragments for SNM discrimination. The corresponding zoom-in spectra of the signal peaks of these three fragments for the eight SNMs are shown in Fig. 3(d-f). The decay information of the three fragments is listed in Tab. 1. To better reflect the actual detection results, a detailed analysis of the statistical sources of the characteristic peaks is also performed in Tab. 1. It is divided into two aspects, one is the delayed γ peaks of other nuclides with energy close to the characteristic peaks (which the resolution of the detector is inadequate to distinguish), and second, some neutron-rich nuclei through β decay to the identified nuclides within the detection time. For example, for the nuclide ^{94}Y which has a half-life of 18.7 minutes, the nuclides ^{94}Sr, ^{94}Rb, ^{94}Kr, and ^{94}Br can all produce ^{94}Y through β decay within the detection time. At this point, the yield of ^{94}Y calculated from the counts of the characteristic peak is the sum of the yields of these nuclides. The last column of Tab. 1 indicates the productivities of these interested fragments (the probability of one γ photon generating this nuclide at 14 MeV), which can provide a quantitative standard for the high yield of fragments. These nuclides form three pairs of fragment identification ratio, ^{94}Y/^{89}Rb, ^{138}Cs/^{98}Rb, ^{138}Cs/^{94}Y, among which the first one requires the least measurement time.
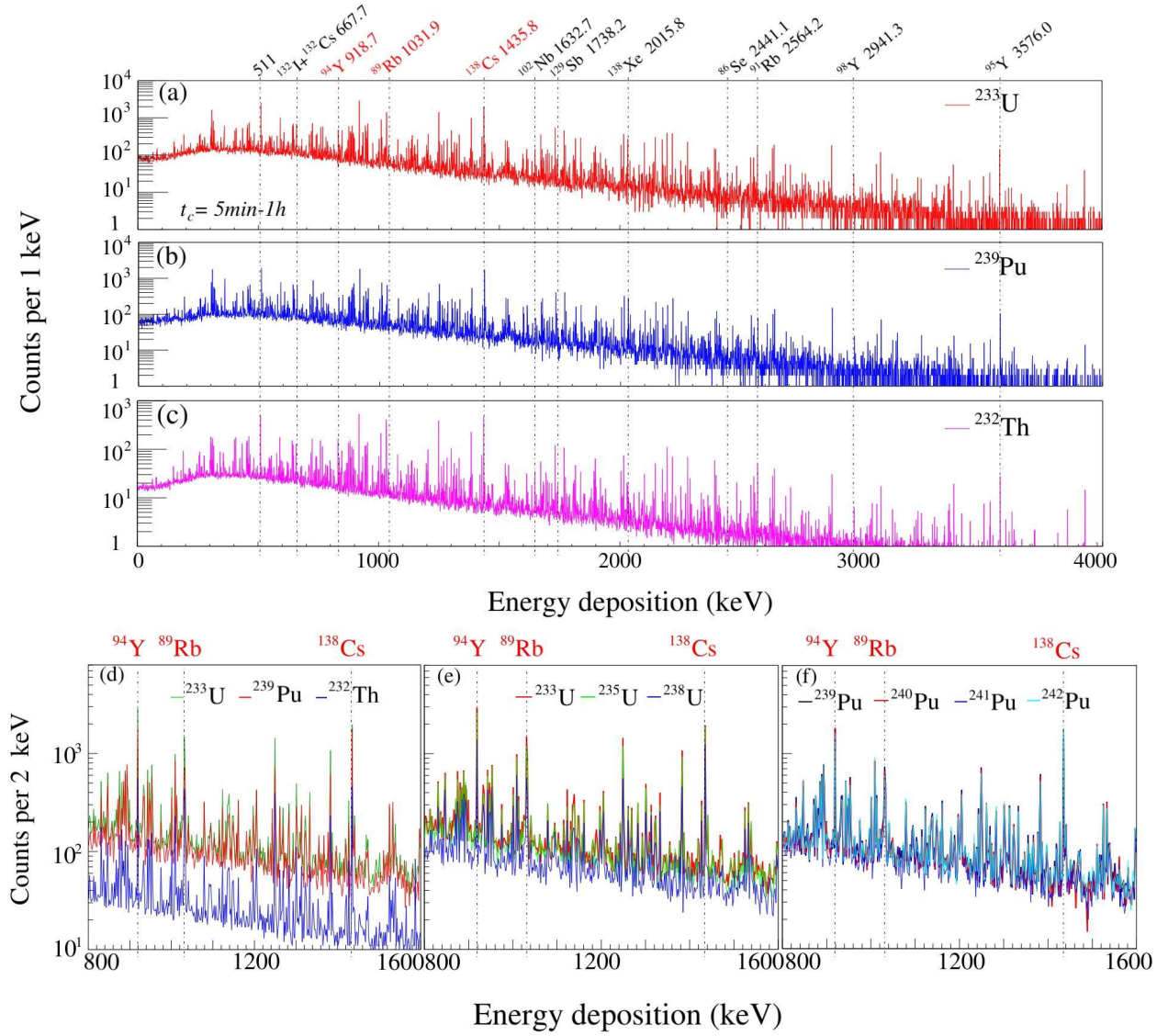
Fig. 3. (a), (b), and (c) are the exemplary full γ ray spectra recorded by the HPGe detector from fission fragments of the SNM isotopes ^{233}U, ^{239}Pu, and ^{232}Th, respectively. The peak positions of the characteristic delayed γ signals for the candidate high-yield fission fragments are labelled with black dashed lines. (d), (e), and (f) are the zoom-in spectra of the delayed γ signals from the eight SNM isotopes. The incident γ ray energy is 14 MeV.

TABLE 2. The calculated counts, yield ratios along with the associated statistical uncertainty for three pairs of nuclides. The incident γ-ray energy is 14 MeV.

| Fissile nucleus	Net counts			Yield ratio		
	^{138}Cs	^{89}Rb	^{94}Y	^{138}Cs / ^{89}Rb	^{138}Cs / ^{94}Y	^{94}Y / ^{89}Rb
^{233}U	1788	1350	1731	1.168±0.04	0.747±0.03	1.563±0.06
^{235}U	1567	1126	1556	1.324±0.05	0.837±0.03	1.582±0.06
^{238}U	1130	505	776	1.953±0.10	1.207±0.06	1.618±0.09
^{239}Pu	1603	625	1032	2.207±0.10	1.124±0.04	1.963±0.10
^{240}Pu	1506	573	1026	2.416±0.12	1.210±0.05	1.996±0.10
^{241}Pu	1344	487	831	2.509±0.13	1.322±0.06	1.898±0.11
^{242}Pu	1635	500	856	2.906±0.15	1.546±0.07	1.880±0.11
^{232}Th	424	407	325	1.014±0.06	1.067±0.06	0.950±0.06
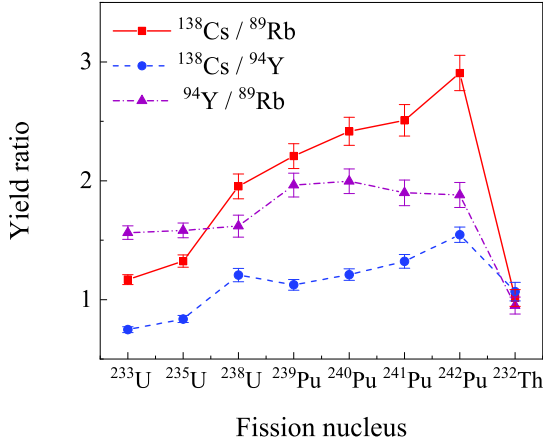
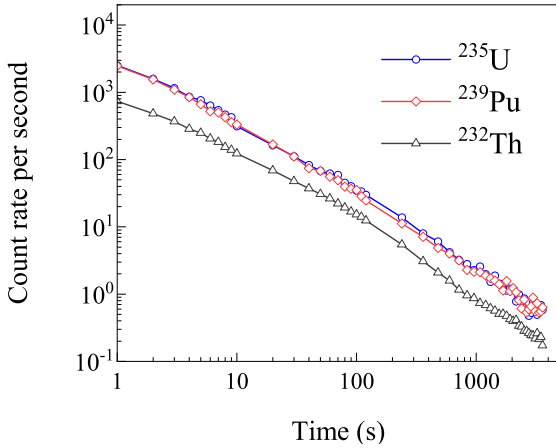Fig. 4. The fragment ratio yields for the eight SNMs at the incident γ energy of 14 MeV.

Fig. 5. The count rate of delayed γ above 3 MeV recorded by the LaBr$_3$ detector between 1 to 1000 seconds after the fission reactions of U, Pu, and Th.

C. Yield Analysis

Considering the differences in actual detection conditions, such as measurement time variations and interrogation source energy, this work utilizes the yield ratio as a more convenient and generalized basis for SNM identification. According to the delayed γ spectra recorded by the HPGe detector, the characteristic γ counts are calculated by subtracting the backgrounds ± 1 keV around the peak from the gross counts. The specific values of the obtained counts and the yield ratios are given in Tab. 2. The yields are then calculated from the net counts considering the delayed γ-ray intensity, detection efficiency, and target attenuation. The uncertainties of the yields and their ratios are obtained by performing least-squares fitting on the statistical error of the counts. As shown in Tab. 2, the net counts of ^{89}Rb are lower than those of ^{94}Y and ^{138}Cs,

making the relative uncertainty of the yield ratios involving ^{89}Rb higher than that of ^{138}Cs/^{94}Y.

The yield ratios of three pairs of nuclides, consisting of the finally selected fragment nuclides ^{138}Cs, ^{94}Y, and ^{89}Rb, are used as the indicator for identifying the selected SNM isotopes, as shown in Fig. 4. The confidence level is calculated to judge whether they can be distinguished from each other within the uncertainty. The yield ratio of ^{138}Cs/^{89}Rb shows a large difference among the SNMs, which can be used to distinguish the other seven nuclides except for $^{239-241}$Pu, with a high confidence level above 99.5%. Although the ^{94}Y/^{89}Rb ratio does not exhibit significance among the isotopes of U, Pu, and Th, it can be used to perform a quick elemental identification. For the isotopes of Pu, the yield ratio of ^{138}Cs/^{94}Y is the most suitable for isotopic discrimination. This pair of nuclides exhibits the smallest uncertainty in the yield ratio and highlights the most noticeable differences among the fission nuclei, especially for $^{239-241}$Pu. However, the ^{138}Cs/^{94}Y ratios of ^{240,241}Pu are close and can not be distinguished. When the total number of the incident γ rays is increased to 10^{11}, these isotopes of Pu can be distinguished by the yield ratio of ^{138}Cs/^{89}Rb and ^{94}Y/^{89}Rb, with a high confidence level above 99.5%. Moreover, ^{138}Cs has a half-life of 33 minutes and thus requires a longer measurement time.

D. High Energy γ Counting Rate

High energy γ rays above 3 MeV have high penetration capabilities and they have been observed intensively in those mentioned above delayed γ-ray spectra of photofission fragments of SNMs. For common shielding materials such as Pd and Bi, the photofission (or photo-induced spallation) thresholds are typically above 100 MeV, which are much larger than those of SNMs. When irradiated by γ beam around 14 MeV, these high-Z benign materials would not undergo photofission but common photonuclear reactions such as (γ, xn). The delayed γ rays typically released from the reaction residuals are mostly less than 3 MeV. Consequently, delayed γ rays above 3 MeV from photofission might serve as an effective basis for determining the presence of nuclear material. The γ counts above 3 MeV resulting from fragment decay were recorded by a LaBr$_3$ detector. Fig. 5 shows the change in the counting rate of three elements U, Pu, and Th within 1s-1000s of measurement time. As demonstrated in Fig. 5, the count rates of the three SNM elements exhibit differences, but the difference is within the error range, which is not suitable as a basis for distinguishing between them. As nuclear materials mainly generate high-energy γ rays, so these results can provide data support for identifying whether they are SNMs.

IV. DISCUSSION AND SUMMARY

The variation trends of the three pairs of yield ratios at incident photon beam energies of 10 to 18 MeV are illustrated in Fig. 6. It is observed that the yield ratio is highly dependent on the fission nucleus. As energy increases, the yield ra-
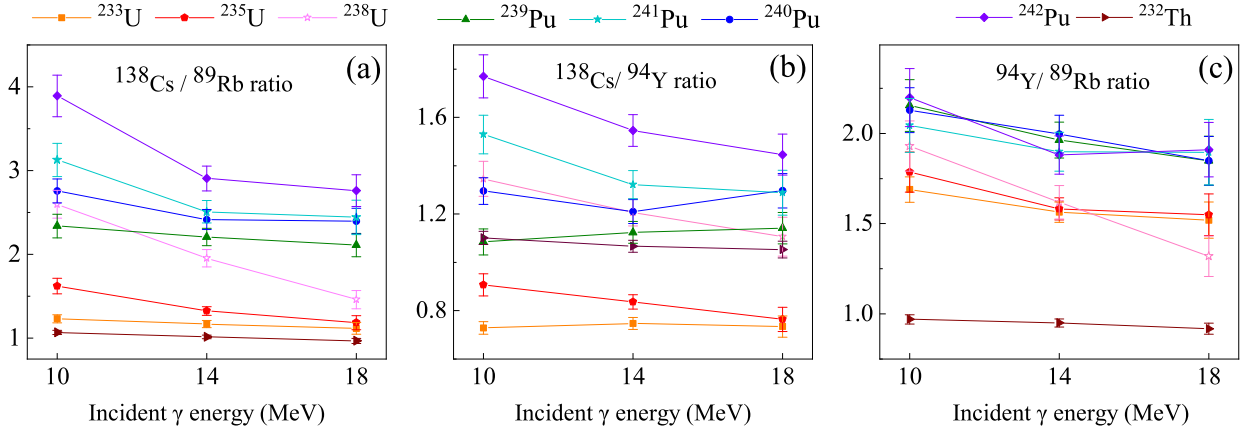
Fig. 6. (a), (b), and (c) are the three yield ratios, ^{138}Cs/^{89}Rb, ^{138}Cs/^{94}Y, and ^{94}Y/^{89}Rb, respectively, for the eight SNMs under the incident photon energy of 10-18 MeV.
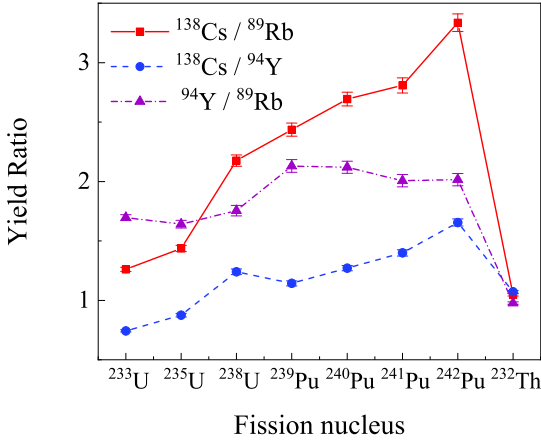

Fig. 7. The yield ratios of photofission on SNMs induced by bremsstrahlung from the interaction of 18 MeV electrons with a tantalum target. An electron charge of 10^{13} is used.
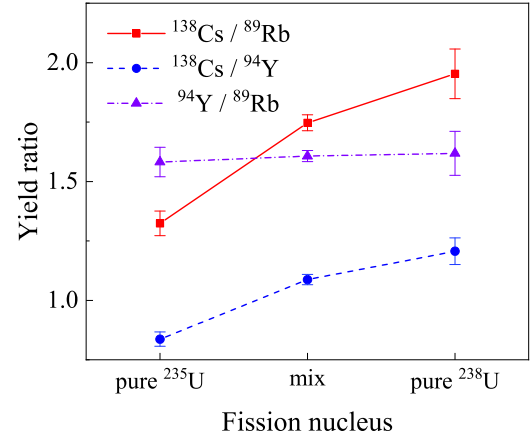

Fig. 8. The yield ratio when the object to be detected is a mixture of ^{235}U and ^{238}U.

tio of ^{138}Cs/^{89}Rb exhibits diminishing differences across various fission nuclei, while the yield ratios of ^{138}Cs/^{94}Y and ^{94}Y/^{89}Rb demonstrate relatively weak dependence on the incident photon beam energy. In short, under the incidence of γ rays of other energies, the method of distinguishing fission nuclei by yield ratio remains effective. When the interrogation source is a bremsstrahlung beam, as illustrated in Fig.7, the identification method proposed in this paper remains applicable [24]. It can be observed that the yield ratios of the three pairs of nuclides exhibit a good identification effect, and the specific values show good consistency with the previous results. Due to the low proportion of γ rays effectively triggering fission reactions in bremsstrahlung, higher-intensity electrons were used to simulate this process. As observed, under higher intensities beam, the yield ratios of the eight nuclides are more distinguishable, leading to improved recognition and higher reliability. Moreover, We also discussed the

identification under a monoenergetic γ beam of 14 MeV for the mixture of uranium isotopes in nuclear fuel, where ^{235}U accounts for 20% and ^{238}U for 80%. The yield ratio results are presented in Fig. 8 below. In this way, the yield ratio of ^{138}Cs/^{89}Rb and ^{138}Cs/^{94}Y can identify the mixture as being made of ^{235}U and ^{238}U. Furthermore, the relative abundances of these isotopes are linearly dependent on the yield ratios. This demonstrates that the detection method remains effective in distinguishing and quantifying isotopes in mixed compositions, thereby extending its applicability to real-world scenarios.

This paper provides the identification method for SNM by utilising the yield ratios of photofission fragments to differentiate among U, Pu, Th, and their isotopes. The simulation of photofission was performed using the self-added photofission module in Geant4, which supplied information on the fission fragments. In the mass and charge yield distribution and decay spectrum of fission fragments, the measurable prod-

uct nuclides that have high yields and differences in SNMs were selected. Identify SNMs through the yield ratio of nuclides, in which $^{239-241}$Pu require a higher intensity γ beam to increase the confidence of the results. The yield ratios of selected product nuclides in different energies of the incident photon beams show good stability and discrimination. In the photofission induced by bremsstrahlung, the identification method is equally effective. This result indicates that the identification method proposed in this work is minimally affected by the light source, providing substantial feasibility and reliability for the widespread application of real SNM detection in the future. In addition, our laboratory has successfully detected short-lived isotopes with a half-life of 40 ms, and this provides an experimental and theoretical foundation for the future realisation of fast identification of SNMs.

[1] R.T. Kouzes, E.R. Siciliano, J.H. Ely, *et al.*, Passive neutron detection for interdiction of nuclear material at borders. Nucl. Instr. Meth. A **584**, 383-400 (2008). doi: 10.1016/j.nima.2007.10.026

[2] D. Cester, G. Nebbia, L. Stevanato, *et al.*, Special nuclear material detection with a mobile multi-detector system. Nucl. Instr. Meth. A **663**, 55-63 (2012). doi: 10.1016/j.nima.2011.10.011

[3] C.F. Zhang, Q.P. Xiang, R.D. Ze, *et al.*, An enhanced method of neural network algorithm with multi-coupled gamma and neutron characteristic information for identifying plutonium and uranium. Nucl. Instr. Meth. A **996**, 165128 (2021). doi: 10.1016/j.nima.2021.165128

[4] D.F. Tian, D. Xie, Y.K. Ho, *et al.*, Fissile material isotopic composition by γ-ray spectra. Nucl. Instr. Meth. A **449**, 500-504 (2000). doi: 10.1016/S0168-9002(99)01472-2

[5] D.G. Beddingfield, E.E. Cecil, Identification of fissile materials from fission product gamma-ray spectra. Nucl. Instr. Meth. A **417**, 405-412 (1998). doi: 10.1016/S0168-9002(98)00781-5

[6] R.E. Marrs, E.B. Norman, J.T. Burkeetal, Fission-product gamma-ray line pairs sensitive to fissile material and neutron energy. Nucl. Instr. Meth. A **592**, 463-471 (2008). doi: 10.1016/j.nima.2008.04.032

[7] A. Iyengar, E.B. Norman, C. Howard, *et al.*, Distinguishing fissions of ^{232}Th, ^{237}Np and ^{238}U with beta-delayed gamma-rays. Nucl. Instr. Meth. B **304**, 11-15 (2013). doi: 10.1016/j.nimb.2013.03.054

[8] M. Tohamy, J.M. Crochemore, K. Abbas, *et al.*, Identification of short-lived fission products in delayed gamma-ray spectra for nuclear material signature verifications. Nucl. Instr. Meth. A **978**, 164347 (2020). doi: 10.1016/j.nima.2020.164347

[9] X.Y. Pan, Y.F. Zheng, Z. Zeng, *et al.*, Experimental validation of material discrimination ability of muon scattering tomography at the TUMUTY facility. Nucl. Sci. Tech. **30**, 120 (2019). doi: 10.1007/s41365-019-0649-4

[10] L.J. Hou, Q.H. Zhang, J.Q. Yang, *et al.*, A novel reconstruction algorithm based on density clustering for cosmic-ray muon scattering inspection. Nucl. Eng. Technol. **53**, 2348-2356 (2021). doi: 10.1016/j.net.2021.01.014

[11] W.B. He, D.Y. Chang, R.G. Shi, *et al.*, Material discrimination using cosmic ray muon scattering tomography with an artificial neural network. Radiat. Detect. Technol. Methods. **6**, 254–261 (2022). doi: 10.1007/s41605-022-00319-3

[12] F.L. Liu, H.R. Wang, N. Bo, *et al.*, Proof-of-principle Study of Explosive Detection Based on Nuclear Resonance Absorption. Atom. Energ. Sci. Tech. **56**, 258-264 (2022). doi: 10.7538/yzk.2022.youxian.015

[13] H. Y. Lan, T. Song, J. L. Zhang, *et al.*, Rapid interrogation of special nuclear materials by combining scattering and transmission nuclear resonance fluorescence spectroscopy. Nucl. Sci. Tech. **32**, 84 (2021). doi: 10.1007/s41365-021-00914-x

[14] H.Y. Lan, T. Song, Z.H. Luo *et al.*, Isotope-sensitive imaging of special nuclear materials using computer tomography based on scattering nuclear resonance fluorescence. Phys. Rev. Appl. **16**, 054048 (2021). doi: 10.1103/PhysRevApplied.16.054048

[15] H.Y. Lan, T. Song, X.D. Huang *et al.*, Nuclear resonance fluorescence drug inspection. Sci. Rep. **11**, 1306 (2021). doi: 10.1038/s41598-020-80079-6

[16] E. Simon, F. Jallu, B. Pérot, *et al.*, Feasibility study of fissile mass quantification by photofission delayed gamma rays in radioactive waste packages using MCNPX. Nucl. Instr. Meth. A **840**, 28-35 (2016). doi: 10.1016/j.nima.2016.09.047

[17] M. Delarue, E. Simon, B. Pérot, *et al.*, New measurements of cumulative photofission yields of ^{239}Pu, ^{235}U and ^{238}U with a 17.5 MeV bremsstrahlung photon beam and progress toward actinide differentiation. Nucl. Instr. Meth. A **1040**, 167259 (2022). doi: 10.1016/j.nima.2022.167259

[18] F. Carrel, M. Agelou, M. Gmar, *et al.*, Identification and differentiation of actinides inside nuclear waste packages by measurement of delayed gammas. IEEE Trans. Nucl. Sci. **57**, 2862-2871 (2010). doi: 10.1109/TNS.2010.2064334

[19] F. Carrel, M. Gmar, F. Laine, *et al.*, Identification of actinides inside nuclear waste packages by measurement of fission delayed gammas. IEEE Nuclear Science Symposium Conference Record **28-1**, 909-913 (2006). doi: 10.1109/NSS-MIC.2006.355994

[20] I.V. Pylypchynets, O.O. Parlag, V.T. Maslyuk, *et al.*, Isotopic identification of photofissed nuclear materials in stainless steel containers using delayed amma-rays. Probl. Atom. Sci. Tech. **5**, 103-109 (2022). doi: 10.46813/2022-141-103

[21] H.L. Liu, H.B. Ji, JM Zhang, *et al.*, Novel algorithm for detection and identification of radioactive materials in an urban environment. Nucl. Sci. Tech. **34**, 154 (2023). doi: 10.1007/s41365-023-01304-1

[22] S. Qi, S.Q. Wang, Y. Chen, *et al.*, Radionuclide identification method for NaI low-count gamma-ray spectra using artificial neural network. Nucl. Eng. Technol. **54**, 269-274 (2022). doi: 10.1016/j.net.2021.07.025

[23] C.L. Hollas, D.A. Close, C.E Moss, Analysis of fissionable material using delayed gamma rays from photofission. Nucl. Instr. Meth. B **24-25**, 503-505 (1987). doi: 10.1016/0168-583X(87)90695-1

[24] S.W. Finch, M. Bhike, C.R. Howell, *et al.*, Measurements of short-lived isomers from photofission as a method of active interrogation for special nuclear materials. Phys. Rev. Appl. **15**, 034037 (2021). doi: 10.1103/PhysRevApplied.15.034037

[25] L.X. Liu, H.W. Wang, G.T. Fan, *et al.*, The SLEGS beamline of SSRF. Nucl. Sci. Tech. **35**, 111 (2024). doi: 10.1007/s41365-024-01469-3

[26] H.W. Wang, G.T. Fan, L.X. Liu, *et al.*, Commissioning of laser electron gamma beamline SLEGS at SSRF. Nucl. Sci. Tech. **33**, 87 (2022). doi: 10.1007/s41365-022-01076-0

[27] J. X. Liu, H. Y. Lu, H. G. Lu, *et al.*, Generation of ~400

pC electron bunches in laser wakefield acceleration utilizing a structured plasma density profile. Phys. Plasmas **30**, 113103 (2023). doi: 10.1063/5.0161811

[28] D. Wu, H. Y. Lan, J. X. Liu, *et al.*, Ultra-short lifetime isomer studies from photonuclear reactions using laser driven ultra-intense γ-ray. (2023). arxiv: 2402.15187

[29] D. Wu, H. Y. Lan, J. Y. Zhang, *et al.*, ^{197}Au(γ, xn; x = 1 $\sim$ 7) reaction measurements using laser-driven ultra-bright ultra-fast bremsstrahlung γ-ray. (2023). arxiv: 2209.13947

[30] D. Wu, H. Y. Lan, J. Y. Zhang, *et al.*, New measurements of ^{92}Mo(γ, n) and (γ, 3n) reactions using laser-driven bremsstrahlung γ-ray. Front. Phys. **11**, 1178257 (2023). doi: 10.3389/fphy.2023.1178257

[31] Z.C. Li, Y. Yang, Z.W. Cao, *et al.*, Effective extraction of photoneutron cross-section distribution using gamma activation and reaction yield ratio method. Nucl. Sci. Tech. **34**, 170 (2023). doi: 10.1007/s41365-023-01330-z

[32] J.Y. Z., D. Wu, H.Y. Lan, *et al.*, Generation of medical isotopes ^{47}Sc, ^{67}Cu through laser-induced (γ, p) reaction. Nucl. Sci. Tech. **35**, 206 (2024). doi: 10.1007/s41365-024-01550-x

[33] M.Z. Wang, D. Wu, H.Y. Lan, *et al.*, Cross section measurements of ^{27}Al(γ, x)^{24}Na reaction as monitors for laser-driven bremsstrahlung γ-ray. Nucl. Phys. A **1043**, 122834 (2024). doi: 10.1016/j.nuclphysa.2024.122834

[34] F.L. Liu, C.Y. He, H.R. Wang, *et al.*, Thick-target yield of 17.6 MeV γ ray from the resonant reaction ^{7}Li(p, γ)^{8}Be at E_p = 441 keV. Nucl. Instr. Meth. B **529**, 56-60 (2022). doi: 10.1016/j.nimb.2022.08.005

[35] Y.L. Dang, F.L. Liu, G.Y. Fu, *et al.*, New measurement of thick target yield for narrow resonance at E_x=9.17 MeV in the ^{13}C(p,γ)^{14}N reaction. Chin. Phys. B **28**, 060706 (2019). doi: 10.1088/1674-1056/28/6/060706

[36] S. Agostinelli, J. Allison, K. Amako, *et al.*, Geant4—a simulation toolkit. Nucl. Instr. Meth. B **506**, 3 (2003). doi: 10.1016/S0168-9002(03)01368-8

[37] X.M. Shi, G. L. Wang, K. J. Luo, *et al.*, Geant4 development for actinides photofission simulation. Nucl. Instr. Meth. A **1062**, 169222 (2024). doi: 10.1016/j.nima.2024.169222

[38] G. L. Wang, H. Y. Lan, X. M. Shi, *et al.*, A general framework for describing photofission observables of actinides at an average excitation energy below 30 MeV. Chinese Phys. C **46**, 084102 (2022). doi: 10.1088/1674-1137/ac6abc

[39] D.M.Gorodisskiy, K.V.Kovalchuk, S.I.Mulgin *et al.*, Systematics of fragment mass yields from fission of actinide nuclei induced by the 5–200 MeV protons and neutrons. Ann. Nucl. Energ. **35**, 328-245 (2008). doi: 10.1016/j.anucene.2007.06.002

[40] A.J. Koning, D. Rochman, J.-Ch. Sublet *et al.*, TENDL: Complete Nuclear Data Library for Innovative Nuclear Science and Technology. NUCL. DATA SHEETS **155**, 1-55 (2019). doi: 10.1016/j.nds.2019.01.002